

Characterizing the Absolute Quantum Efficiency of SNAP NIR Photodetectors

Anastasia Karabina

Advisor: Wolfgang Lorenzon

A Thesis presented for the degree of
Bachelor of Science

SNAP Group
Department of Physics
University of Michigan
April 2008

Dedicated to

My parents, for all the support they have given me in every thing I have ever tried, for their endless encouragement through my successes and especially through my struggles, for always being proud of me for exactly who I am, and because no matter what I do or how things turn out, I know that they will always be there, loving me unconditionally. I love you Mom and Dad.

Characterizing the Absolute Quantum Efficiency of SNAP NIR Photodetectors

Anastasia Karabina

Submitted for the degree of Bachelor of Science
April 2008

Abstract

Dark energy is accelerating the expansion of the universe. The SuperNova Acceleration Probe (SNAP) is a proposed spaced based telescope with the goal of measuring the expansion of the universe and characterizing the nature of dark energy. NIR detectors present on SNAP must be tested and characterized for many parameters. One such parameter is the absolute quantum efficiency. The University of Michigan SNAP NIR laboratory is working on characterizing the quantum efficiency of space grade NIR detectors. This thesis will present the experimental setup and procedure for taking an absolute quantum efficiency measurement. An analysis of the QE system parameters is thoroughly discussed. The effects of QE system parameters are related to the QE data produced. The QE measurements for H2-103 show that the device is capable of producing an average QE of 80% for wavelengths 1000 – 1700nm.

Declaration

The work in this thesis is based on research carried out by the University of Michigan SNAP group, in the Department of Physics at the University of Michigan, Ann Arbor. No part of this thesis has been submitted elsewhere for any other degree or qualification and is all my own work unless referenced to the contrary in the text.

Copyright © 2008 by Anastasia Karabina

“The copyright of this thesis rests with the author. No quotations from it should be published without the author’s prior consent and information derived from it should be acknowledged.”

Acknowledgements

I would not have been able to make it to where I am today without the unlimited help I have received from the following people:

—Wolfgang Lorenzon, my advisor, who has been there every step of the way. I can't stress enough how much I appreciate his guidance, support, and most importantly, the confidence that he has put in me.

—Michael Schubnell, whose endless knowledge and expertise I have counted on to get me from one challenge to the next.

—Greg Tarlé, for his constant cheerful attitude and his ability to see the silver lining in every situation.

—Curtis Weaverdyck, for the countless hours he has spent in the lab teaching me everything from computer procedures to clever shortcuts to handling hardware. Without his mentorship I would not have survived this long.

—Tomasz Biesiadzinski and Matt Brown, for taking the time to help me out, despite their very busy graduate careers.

Contents

	Abstract	iii
	Declaration	iv
	Acknowledgements	v
1	Introduction	1
	SNAP Overview	1
	NIR Detectors	2
2	Experimental Setup	4
3	Experimental Procedure	9
	Preparation.	9
	Test Procedures	9
4	Improvements	12
	Cold Photodiode	12
	GPIB	12
	Uniform Light	13
5	Data Analysis	15
	Quantum Efficiency Measurements	15
	Scattered Light.	17
	Uniform Light	18
	Conversion Gain.	21
	Repeatability.	21
	Bibliography	23

List of Figures

- 1.1 Picture of H2-103, one of the NIR detectors that have been tested in the SNAP laboratory.
- 2.1 Picture demonstrating the system of light characterization for the quantum efficiency setup.
- 2.2 Picture showing details of the black box.
- 2.3 Picture showing the inside of the dewar, and plunger system used to move detector and photodiode during measurements at 140 K.
- 2.4 Picture demonstrating the placement of the cryogenic dewar in the quantum efficiency setup and all of its electronic connections.
- 3.1 Image of a Flexible Image Transport System (FITS) file. FITS is used to store and process images in a digital file format. In the SNAP laboratory FITS files are supported by SAO Image DS9. The FITS image above was taken by H2-103 at peak wavelength 1300 nm. A FITS file represents an array of every pixel value in the detector.
- 4.1 One-dimensional scan showing the light distribution across the plane of the detector before improvements were made to reduce scattered light.
- 4.2 One-dimensional scan showing the light distribution across the plane of the detector after the QE system had been modified.
- 5.1 Format of QE data and header stored in the online database for a recent measurement.
- 5.2 Presentation of data computed for each wavelength in the QE analysis.
- 5.3 Quantum efficiency measurement showing three data sets that were all taken under the same conditions.
- 5.4 Left panel: QE data analyzed using two different dark images. The standard data taking method is in blue, and the data using the new dark measurement is in red.
Right Panel: The ratio of the two QE curves. The agreement of the two curves provides strong evidence that scattered light in the QE system has been eliminated.
- 5.5 Photodiode current at three wavelengths, 1000 nm, 1300 nm, and 1680nm, for four different vertical positions. The photodiode current is independent of position.
- 5.6 QE measurements at three wavelengths, 1000 nm, 1300 nm, and 1680nm, for four different vertical positions. The graph shows that the QE is independent of position.
- 5.7 Comparison of two color QE Maps at different positions. The PD current was the same for both measurements. From the comparison, it can be concluded that the light distribution does not vary with position and is therefore a flat field for the current test conditions.
- 5.8: An image showing the subtraction of two QE images taken at different positions. The smoothness of the image demonstrates a uniform light field.
- 5.9 Plot of a conversion gain measurement. Three data points were computed from the mean and variance of three subsections. The slope of these points is the conversion gain.
- 5.10 Measurements of the photodiode current taken over two consecutive days. The data shows a nice consistency

Chapter 1

Introduction

1.1 SNAP Overview

For almost 80 years it has been known that we live in an expanding universe. Until 10 years ago this expansion was believed to be decelerating due to the gravitational forces that dominate our universe. In 1998 there was enough observable evidence to conclude that the rate of expansion of the universe was indeed accelerating. This acceleration is accounted for by dark energy, a concept we know nearly nothing about. Astronomical observations have allowed us to account for about one quarter of the universe's mass-energy density (4% ordinary matter, 22% dark matter); dark energy fills the remaining 74% of the universe's mass-energy budget. Dark matter itself does not radiate any light, therefore it can not be seen. It is not quite as mysterious as dark energy due to the fact that its gravitational effects on astronomical bodies can be observed and thus its quantity can be calculated. Dark natured quantities are considered to be composed of unknown entities, different from any particles currently known in the universe [3].

The SuperNova Acceleration Probe (SNAP) is a telescope designed to measure the expansion of the universe and characterize the nature of dark energy. SNAP will use Type 1a supernovae as standard candles to map the expansion history of the universe [5]. As the light emitted from a supernova travels to the SNAP telescope, the expansion of space stretches its wavelength, and a redshift of the supernova spectrum is observed. Supernovae that are further away have higher redshifts. Eventually their spectra are shifted out of the visible range and into the infrared (IR) range. By surveying supernovae that are further away, SNAP will be able to measure the universe's expansion history back 10 billion years [5]. However, in order to view these spectra, SNAP must have detectors receptive to wavelengths in the IR as well as in the visible.

SNAP will be a 2-meter telescope capable of sampling approximately 2000 Type 1a supernovae. Each image taken by SNAP will be one square degree, an extremely large field of view. The telescope will contain 72 cameras in the focal plane (36 CCDs and 36 NIR detectors) that together are able to detect light ranging from 350 nm to 1700 nm. The University of Michigan SNAP group is responsible for the characterization of the NIR detectors that will be needed for SNAP [6].

1.2 NIR Detectors

The University of Michigan has received HgCdTe NIR detectors from two manufacturers, Raytheon Vision System (RVS) and Teledyne Scientific & Imaging (TSI). The NIR detectors used on SNAP will each consist of a 2048×2048 grid of pixels, each pixel being 18 square μm . It is the responsibility of the Michigan NIR laboratory to obtain 36 science-grade NIR detectors that meet the SNAP requirements by fully characterizing the following:

- Detector Sensitivity
 - Gain
 - Read Noise
 - Dark Current
 - Relative and Absolute Quantum Efficiency
- Detector Uniformity
 - Inter-pixel Response Uniformity
 - Intra-pixel Response Uniformity
 - Response Linearity
 - Lateral Charge Diffusion
- Detector Stability
 - Latent Charge
 - Thermal Stability
- Detector Performance
 - Multiplexer Glow
 - Reset Behavior

Quantum efficiency measures a device's ability to convert incident photons into electron-hole pairs. Ideally every photon that falls on the photosensitive surface of the detector should be converted into one electron-hole pair; this would correspond to 100% QE. Electrons may be ejected from matter if they have absorbed enough energy from an incident photon. This is known as the photoelectric effect, and the emitted electrons are then referred to as photoelectrons. When an incident photon hits a material that has an electrical sensitivity to light, the energy of the photon may be absorbed, and an electron-hole pair is created. This incident photon is known as an interacting photon. The quantum efficiency is given by

$$QE = \eta \cdot QE_i,$$

where η is the quantum yield, and QE_i is the interacting QE. The quantum yield is a measure of how many electrons are generated and collected per interacting photon. In our case, η is always equal to one. QE_i is the probability that an incident photon will be converted to an interacting photon [4].

Quantum efficiency is dependent on wavelength since the energy of a photon is determined by its wavelength. Our goal for the final devices chosen for SNAP is to achieve the

highest absolute QE possible over a range from 1000 nm to 1700 nm; although anything above 80% will suffice. The final characterization for the absolute quantum efficiency must be within a 2% error margin. Intra-pixel variation arises when the QE within a single pixel is not uniform. Inter-pixel variation arises when the QE varies from pixel to pixel. One requirement of SNAP is to achieve a QE with 1% uniformity across the whole detector. This means the standard deviation of the fluctuation of the QE must remain within a 1%.



Figure 1.1: Picture of H2-103, one of the NIR detectors that have been tested in the SNAP laboratory.

Chapter 2

Experimental Setup

A system to measure the absolute quantum efficiency has been built in the UM SNAP laboratory. Every aspect of this system had to be carefully considered and thoroughly understood in order to meet the high precision requirements and low error margin desired for our measurements. Our system has been designed to simulate space-like conditions since the detectors must be tested and characterized in the same environment in which they will be operating.

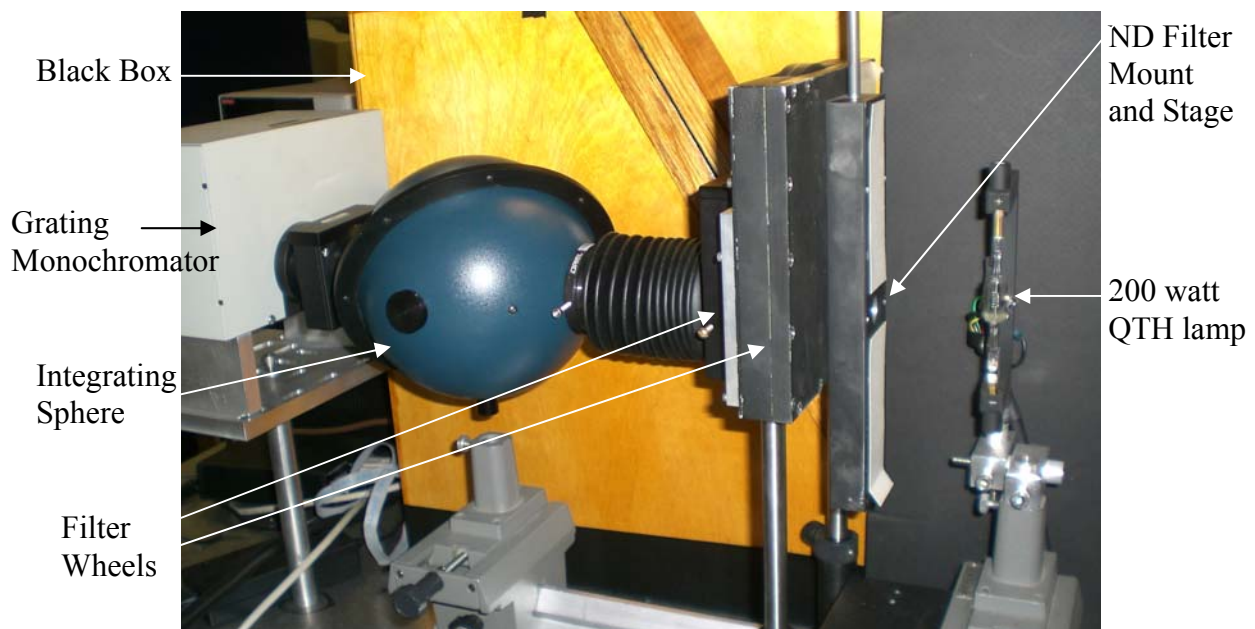


Figure 2.1: Picture demonstrating the system of light characterization for the quantum efficiency setup.

The system starts with a 300 watt radiometric power supply that is hooked up to a light source. The power supply is either hooked up to a 200 watt quartz tungsten halogen (QTH) lamp (model 6332) mounted in front of a filter wheel system, or a 50 watt short filament QTH lamp (model 63368) housed in a PhotoMaxTM hooked up to a grating monochromator. The first

filtering system consists of a four setting manually operated linear stage that is placed in front of two filter wheels, one that holds 12 filters placed in front of one that holds five filters. The purpose of the linear stage is to set a specific transmittance of light that will be used while taking the measurements. The first setting is completely open allowing 100% transmittance of light, the second setting contains a neutral density (ND) filter with an optical density of $d=1.5$, the third contains a 0.5 ND filter, and the last setting is completely blocked allowing no light to reach the detector and photodiode. Neutral density filters are designed to reduce the amount of optical power that passes through it, but more importantly it does so by reducing all wavelengths of light equally. Since our measurements are extremely wavelength dependent this is a necessary feature in our setup. The percentage of transmittance through a ND filter depends on its optical density, d . The fraction transmittance, t_f , is given by

$$t_f = 10^{-d}.$$

Therefore the 1.5 ND filter allows 3.16% of the light through and the 0.5 ND filter allows 31.6% of the light through. If the full intensity of light falls on the detector, the pixels will become saturated. When a pixel becomes saturated it means an amount of light has hit the pixel such that it exceeds the pixel's maximum response value. Quantum efficiency can not be measured if pixels are saturated and therefore ND filters are needed to reduce the overall amount of light hitting the detector. Directly behind the ND filters lies a system of narrow band pass filters that are used to select the light at certain wavelengths. The first position on each of the two wheels does not contain a filter. There are 15 different filters used, each specifying a unique wavelength. Therefore when using filters on the first wheel, the second wheel is set to the first position, and vice versa. The following table provides each filter position with its corresponding wavelength.

Filter 1	Filter 2	Wavelength (nm)	Filter Range (nm)
1	1	Open	
2	1	700	694 – 706
3	1	800	791 – 813
4	1	900	891 – 913
5	1	1000	992 – 1012
6	1	1050	1041 – 1061
7	1	1100	1092 – 1112
8	1	1200	1183 – 1220
9	1	1300	1284 – 1322
10	1	1350	1346 – 1366
11	1	1455	1435 – 1458
12	1	1550	1536 – 1570
1	2	1620	1606 – 1627
1	3	1680	1670 – 1695
1	4	1720	1710 – 1733
1	5	1760	1751 – 1776

Table 2.1: Shows the specific wavelengths tested and their corresponding filter settings when using the filter wheel system for quantum efficiency measurements. The filter range provided gives the cut-off values at a 1% transmittance.

The second light filtering system is a grating monochromator. The monochromator provides a larger range of wavelengths that can be tested, and also produces a much narrower band pass of light. It does this by using diffraction grating to direct a specific wavelength through an exit slit. The specific grating monochromator used is a Spectra-Physics model 77250, which has a usable region of 550 nm to 2000 nm. The wavelength is selected by turning a handle that adjusts the wavelength that passes through the exit slit. A dial that is hooked up to the handle circulates through sequential numbers as it is rotated; the wavelength, λ , being emitted corresponds to the number on the display in the following manner,

$$\text{Number on Display} = \lambda/2 + 9.$$

For example, to emit light at 1000 nm the dial must be turned to 509. The ability of the monochromator to select any wavelength over a continuous range is advantageous. The monochromator has a bandpass of 5-10 nm and is used in situations requiring specific individual wavelengths, spectra and intervals between measurements, when the filters are too broad and cannot reach the needed wavelength.

The filtering system in use is connected to an integrating sphere via a black tube. The integrating sphere is 4 inches in diameter and coated with polytetrafluoroethylene (PTFE) on the inside. An integrating sphere provides a uniform radiance of light out of its exit port through a series of reflections on the inner surface, a necessary element when calculating the quantum efficiency. Keep in mind that to calculate quantum efficiency, two measurements must be obtained: the amount incident light hitting the detector at every pixel, and the amount of light the detector actually detects from every pixel. The latter is easily achieved since the detector provides an exposure of exactly what each pixel sees, the former however is not so easily determined. The method for calculating the amount of incident light hitting the detector depends on a uniform light distribution, and therefore makes having a flat field illumination one of the most critical aspects of the QE setup. The best way to figure out how much light is hitting each pixel in a detector would be for the exact same amount of light to hit every pixel, therefore requiring only one measurement for all pixels. This one measurement comes from the photodiode. The photodiode is located in the same plane as the device, directly below its bottom edge (see Figure 2.3). With a uniform distribution of light across this plane, the amount of light per area assessed by the photodiode is the amount of light per area incident on the detector at every location. If the distribution of light is not a flat field then many tedious calculations must be performed to determine how many photons are hitting the detector in various places. Analyzing quantum efficiency measurements also becomes more of a chore since the relative differences of incoming light presents another variable which must be taken into account.

Light travels from the integrating sphere port into an 18"×19"× 19" (l×w×h) black box. Since it is important that the light remains in a flat field illumination, the box must be light tight and completely black, or in other words, there must be no light leaks or reflections in the box. Each of the edges that come together when the box is closed has 3 grooves in it. The grooves fit into each other when the box is closed, acting as a baffle to prevent light leaks. The box is also completely lined with black material that is very efficient at absorbing infrared light (Figure 2.2).

A cryogenic dewar is secured to the box's exit port. After the light travels the length of the black box, it reaches the dewar window. A NIR detector and a cold calibrated photodiode are located inside the dewar. The dewar is cooled down to 140 K via liquid nitrogen, and kept in a vacuum at approximately 2×10^{-5} torr, thus providing the same environment the detectors will be subjected to on the telescope. The NIR detector and photodiode are mounted on a movable

stage inside the dewar. There is a rod connected to the stage that exits the dewar at the top. The outside portion of the rod has a knob attached to its end. By moving the knob up or down, the stage, the detector and photodiode also move in the vertical direction (Figure 2.3). This pump-like system has a vertical range of about $\frac{3}{4}$ of an inch.



Figure 2.2: Picture showing details of the black box.

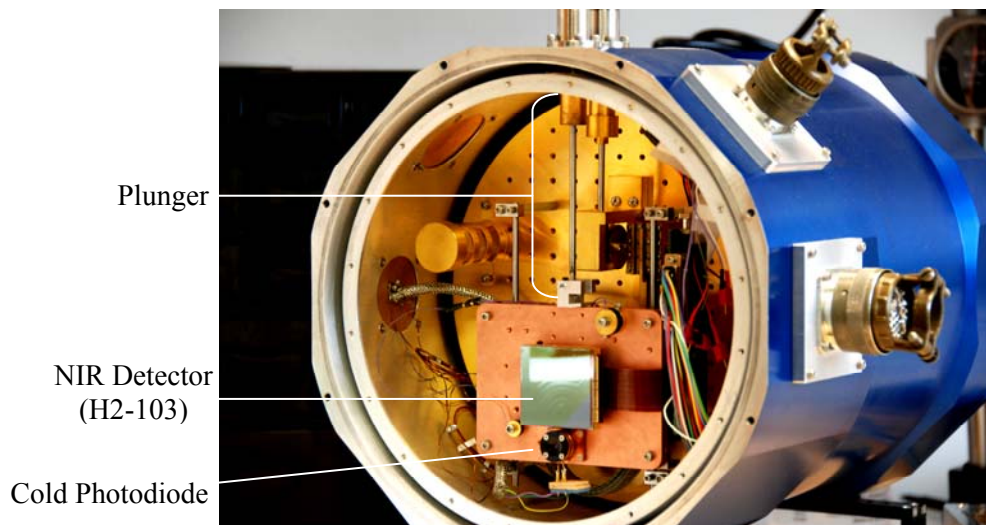


Figure 2.3: Picture showing the inside of the dewar, and the plunger system used to move detector and photodiode during measurements at 140 K.

Measurements of the NIR detector and photodiode are read out by a completely automated computer program, `qe_test_script_gpib.py` found on brainy in `home/daq/devel/Midas/MidasIC/main/Local/Scripts/samples`. The photodiode sends a current to a Keithley 6485 picoammeter, which is then read out by a GPIB and transferred to the computer. When prompted by the computer program an exposure is taken of the NIR detector. The data is read out and sent to the computer by Leach electronics. Once the measurements and images have been generated by the computer program they are ready to be analyzed.

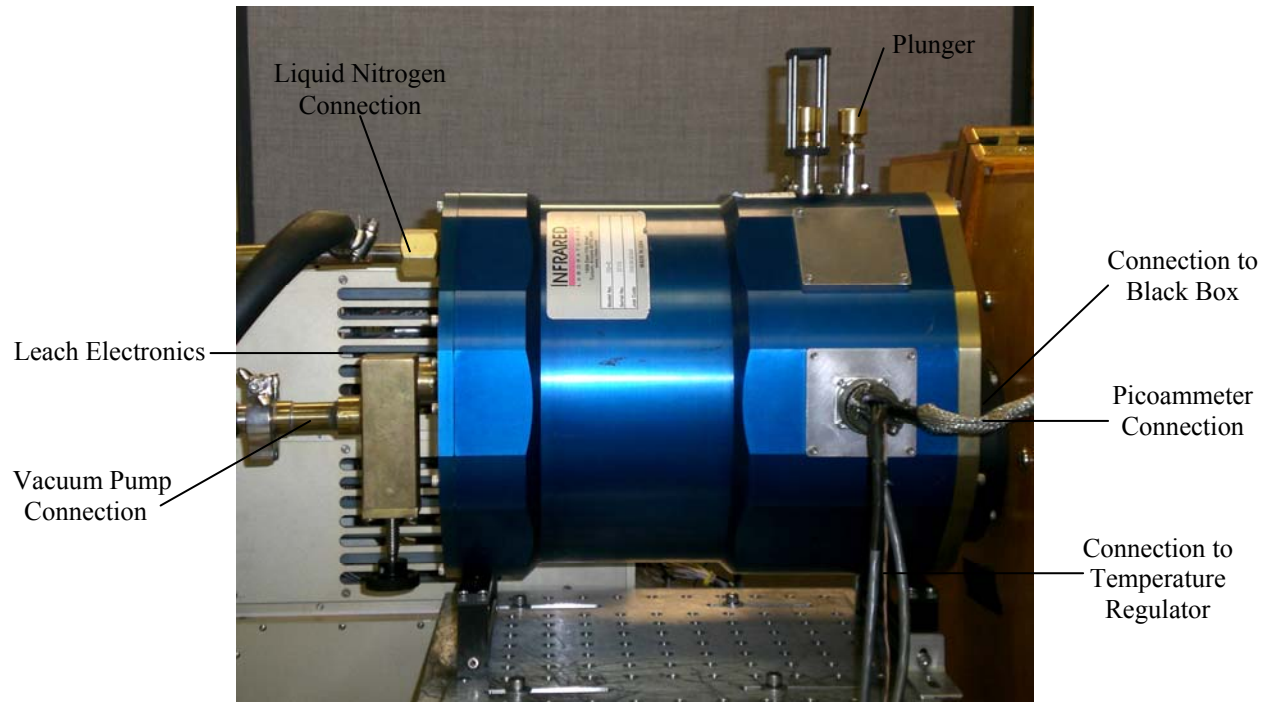


Figure 2.4: Picture demonstrating the placement of the cryogenic dewar in the quantum efficiency setup and all of its electronic connections.

Chapter 3

Experimental Procedure

3.1 Preparation

There is a lot of preparation involved in taking a quantum efficiency measurement. To start, the dewar must be lined up perpendicular to the box's exit port and secured. The dewar must also be hooked up to a vacuum and pumped down to about 2×10^{-5} torr. Next the dewar is hooked up to a liquid nitrogen dewar and cooled down to 140 K. A temperature controller monitors the device and ensures it stays at a steady 140 K by controlling small fluctuations that may occur in the temperature. It takes about 3 hours to pump out the dewar and 4 hours to cool it down, so it is best to do this part of the preparation the day before the quantum efficiency measurements will be taken.

The NIR detector must be hooked up to the Leach electronics, and the photodiode to the picoammeter which is also attached to the GPIB. The Leach electronics and GPIB must be plugged into the computer that will be used to perform the QE measurements. The power supply should be connected to the 200 watt QTH lamp (the default light filtering system) unless the test to be performed requires the monochromator. The light source is ramped up to 6.5 amps for the 200 watt light bulb, and 4.0 amps for the 50 watt light bulb. It is important to let the light source warm up for at least one hour before performing any measurements. This is to make sure the light source has stabilized. The picoammeter must also warm up for an hour. Therefore on the day when a quantum efficiency measurement is going to be performed, at least one hour must be set aside for the preparation alone.

3.2 Test Procedures

After the setup has been prepared, the rest of the procedure for taking a QE measurement is performed almost entirely on the computer. The computer portion of the QE measurements is always the same. There are two computer programs used, the first one (`qe_test_script_gplib.py`) takes all of the actual measurements, and the second program (`AnalyseFits.py` found on gargamel in `/opt/umppy/`) compiles the data into a set of user-friendly graphs and headers. The data for each test is organized in a database categorized first by the device name, secondly by the date of the test, and thirdly by a series number assigned when more than one test is performed in the same day. The set of measurements taken for the first test of a day is labeled series one, and so on.

The first program starts by requesting information about the test to be performed. The device name, the series number of the test for that day, the exposure time of the NIR detector, the wavelength spectrum of the photodiode (infrared or visible), and the temperature of the device are requested first and are characteristics that will belong to every measurement for that test. The program will then prompt, "Take another measurement?" For each measurement taken, the filter number and wavelength of light must be manually entered into the program, while the GPIB automatically enters the photodiode current into the program. An exposure of the NIR detector is taken, and then stored as a FITS file (see Figure 3.1) with a header containing all the information for that measurement. The computer program loops back to the prompt, "Take another exposure?" after each measurement is completed. The actual data gathering portion is completed once all the desired measurements for the test have been taken. All the FITS files that are created are then sorted into the database. Each set of exposures for a test are assigned their own folder based on the series number of the test.



Figure 3.1: Image of a Flexible Image Transport System (FITS) file. FITS is used to store and process images in a digital file format. In the SNAP laboratory FITS files are supported by SAO Image DS9. The FITS image above was taken by H2-103 at peak wavelength 1300 nm. A FITS file represents an array of every pixel value in the detector.

The second program requires much less work. All that must be entered into this program is the device name, the series number, and the date. With this information, the program can find the specified set of measurements within the database. The program then computes the quantum efficiency of each measurement, producing an image and a graph for each wavelength measured. A summary graph of the QE versus wavelength is also produced.

An important part of the quantum efficiency measurements are the dark images. A dark image refers to the image that is taken of the detector when no light is falling on it. If no light is entering the device, there should be nothing to measure, but small amounts of charge are randomly produced and recorded as small electric currents through the device even when there no light is entering the device. This is known as the dark current. Since there is always dark current and background signal noise produced in the device, a dark exposure must be taken. This exposure is assigned a filter number of 99 and a wavelength of 0 in the first computer program. The second computer program subtracts the dark image from all the other images in the series. It is therefore necessary to perform a dark exposure for each series of data.

There are two tests which will be analyzed in this thesis. The first test involves measuring the QE versus the vertical position of the NIR detector and photodiode. The purpose of this measurement is to test whether the light hitting the detector is actually a flat field illumination. Using $\frac{1}{8}$ inch increments there will be seven different positions to measure, starting at 0 inches and ending at $\frac{3}{4}$ inches raised. As the position of the detector and photodiode move with each measurement, the dark image may also change. This means a dark image must be taken for each position, and therefore each position will have to be a new series of measurements. Since this test does not depend on wavelength, all seven series of measurements only need to be taken at one wavelength. I chose 1300 nm because it is near the middle of the NIR spectrum that the detectors are tested over. Each series will only have two exposures, a dark image and an image at 1300 nm. Between each exposure, the QE setup has to be slightly modified for the next measurement; this is the only part of the procedure (besides the preparation) that is not done on the computer. For each dark image, the neutral density filter stage must be set to blocking. For each image at 1300 nm, it must be set to 1.5 ND, with the big filter set to position 9 and the small filter to position 1. Between each series of measurements the detector and photodiode must be raised $\frac{1}{8}$ inch. Once the exposures have been taken, each series must be sorted and evaluated separately.

The second test measures the QE versus wavelength, the default test performed for each device. This test only requires one series of data to be collected. The exposures should be taken in the order of increasing wavelength, with the dark image first. The dark image is the only exposure that requires the ND filters to be changed. For the dark image, the ND filters are set to blocking, and for the rest of the exposures it is set to 1.5 ND. Other than that, the only thing that needs to be modified between each exposure is the filter in use (refer to Table 2.1). The filter number for the dark image is always 99. The filter number for the first illuminated exposure is two, and then the filter number increases sequentially with each new wavelength. There are a total of 16 exposures produced in this test which measure the QE over 15 different wavelengths from 700 nm to 1760 nm.

Chapter 4

Improvements

4.1 Cold Photodiode

There have been many improvements made to the quantum efficiency setup over the last two years. The most significant of these improvements was the replacement of a warm photodiode with a cold-calibrated photodiode. The old photodiode used to be mounted inside the black box since it could not operate at the low temperatures inside the dewar. This made the process of measuring quantum efficiency much more problematic. The photodiode measurement and exposure of the NIR detector had to be performed separately because, while the photodiode was in place, it would obviously scatter and/or block light traveling to the detector. Measurements of the photodiode were taken first. The current for each filter had to be recorded and later entered into the computer program. To remove the photodiode, the box had to be opened between photodiode measurements and exposures. It also had to be disconnected from the picoammeter, which it was connected to through a hole in the box that had been made light tight and re-sealable. The extra work added to the procedure was unfavorable but not the main dilemma. The margin of uncertainty in the QE calculations was much greater due to the QE setup having to be re-arranged in the middle of the measurements and an increased time period between corresponding photodiode and detector measurements.

The difference of location of the photodiode and the NIR detector required further calculations and maintenance. The distance from the light source to the photodiode had to be measured for each new set of data since the photodiode was remounted each time. This distance is necessary to calculate the amount of light at the detector's surface. An even bigger problem arises when the light passes through the dewar window. Light levels vary from outside to inside the dewar due to reflections at the window surface. This required a window transmittance calculation to be performed. Additionally, moisture that may condense on the dewar window or dust that may accumulate could throw off our QE measurements and therefore had to be monitored. Many corrections that required thorough consideration were eliminated by the addition of a cold photodiode, making the QE measurements more accurate and easier to perform.

4.2 GPIB

The photodiode is read out by a very sensitive picoammeter. A typical reading of the photodiode is of order magnitude 10^{-12} A. Fluctuations in the current make it hard to get an accurate reading from the picoammeter display at such small scales. Since the photodiode current directly relates to the quantum efficiency measurement it is important to get the most accurate reading possible. A GPIB was installed and programmed to automate the process of inserting the picoammeter current into our test scripts. After installing the GPIB, I set up a program which takes 10 consecutive readings of the picoammeter and averages them. The 10 values read out by the GPIB have already been averaged by the picoammeter also. This final averaged value is then automatically inserted into the QE scripts. The addition of the GPIB eliminates the possibility of human error while reducing error due to electrical fluctuations by computing an averaged value of the photodiode current.

4.3 Uniform Light

Light leaves the integrating sphere as a flat field illumination and must remain a flat field until it reaches the NIR detector. Light leaks and reflections causing the light distribution to stray from a flat field could only arise in the black box and the 3 inch stretch from the dewar window to the detector. It is important to test whether the light at the plane of the detector is indeed a flat field. With the addition of the cold photodiode also came the installation of a new black box. Therefore tests had to be run to measure the uniformity of the light distribution at the plane of the detector with the newly re-modeled QE system.

A linear motorized stage controlled through a computer program was connected inside the cryogenic dewar. A warm photodiode was mounted on the stage. By taking photodiode measurements at various positions in the dewar, I was able to show a one dimensional light distribution across the plane where the detector lies (see Figures 4.1 and 4.2). The stage could then be moved to show the light distribution in the second dimension of the plane. A continuous measurement of the photodiode could be taken as the motorized stage moved from one end of the dewar window to the other. After performing the test, it was obvious that there was scattered light in our system. The light distribution varied by more than 4% (Figure 4.1). Improvements had to be made until a flat field illumination resulted from the measurements.

The task at hand was to repeat the measurement numerous times, each time altering only one aspect of the black box. This allowed us to see the individual effect that each alteration had on the light distribution. Using this method, reflections were reduced and improvements were made one step at a time. The use of an infrared viewer helped me to further understand how light was being scattered within the system. Baffles at the box's ports were perfected, and the black box was recoated with a new black felt material that is better able to absorb infrared light. After repeatedly modifying the QE system, the light distribution across the whole plane of the detector was reduced to within 0.5% (Figure 4.2).

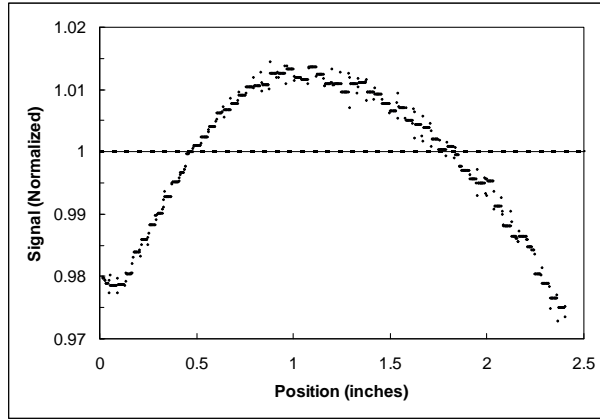


Figure 4.1: One-dimensional scan showing the light distribution across the plane of the detector before improvements were made to reduce scattered light.

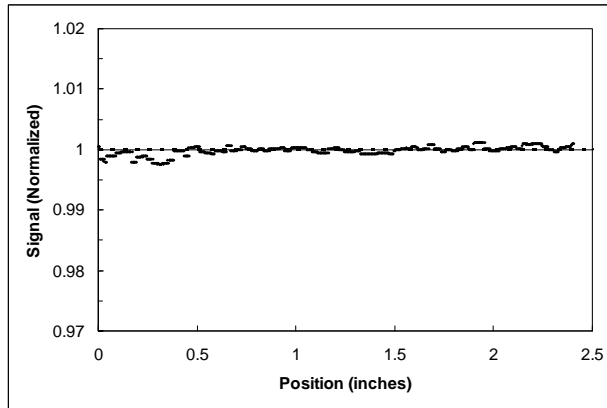


Figure 4.2: One-dimensional scan showing the light distribution across the plane of the detector after the QE system had been modified.

Chapter 5

Data and Analysis

5.1 Quantum Efficiency Measurements

The results from a quantum efficiency measurement are stored on an online database. All measurements are stored in the same format (see Figures 5.1 and 5.2). At the top of the page is a plot of the average QE values at each wavelength, along with a header stating the specific parameters of the measurement (Figure 5.1). The individual measurements performed at each wavelength are presented below this compilation (Figure 5.2). For each wavelength there is a histogram and statistical calculations of the number of pixels at each specific QE value. A color map demonstrating the QE value for each individual pixel across the detector is also presented.

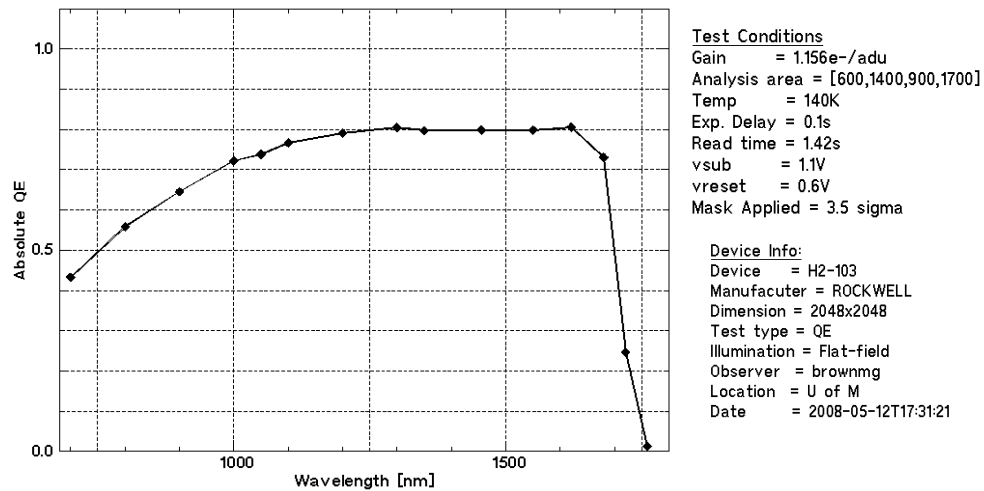


Figure 5.1: Format of QE data and header stored in the online database for a recent measurement.

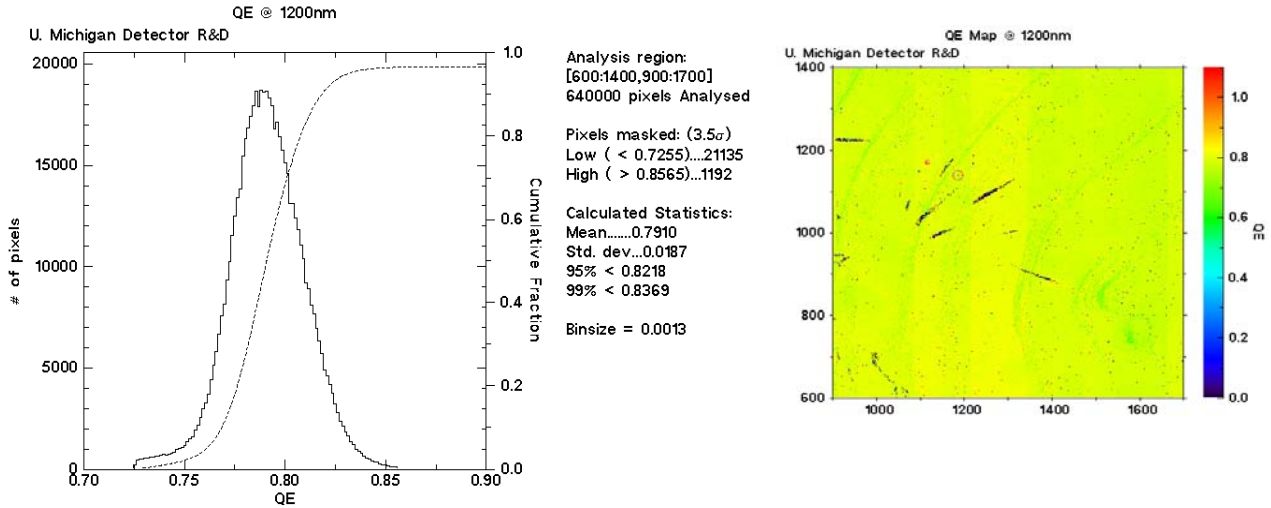


Figure 5.2: Presentation of data computed for each wavelength in the QE analysis.

Quantum efficiency measurements for our newest device, H2-103, are shown in Figure 5.3. The analysis has been performed on a subsection of the detector. The detectors tested in the SNAP lab all come with an anti-reflection (AR) coating. However for this device one corner remained uncoated (this can be seen in Figure 3.1). If a subsection is not defined when analyzing the readout of the detector, the uncoated portion of the detector will skew the overall value of the QE at each wavelength.

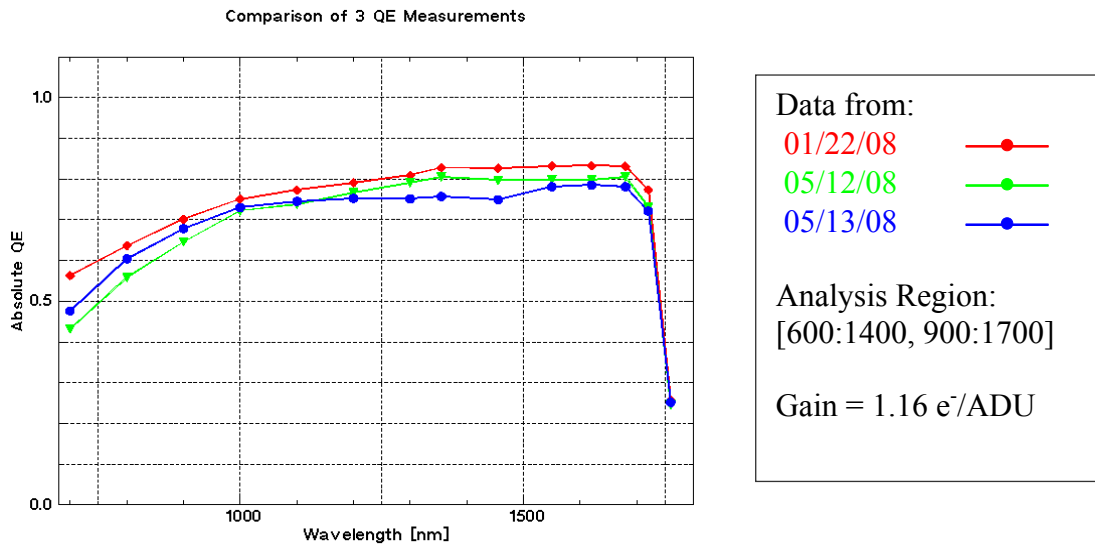


Figure 5.3: Quantum efficiency measurement showing three data sets that were all taken under the same conditions.

The results show a QE between 70-80% for the desired range of wavelengths. This value is slightly low. An important aspect of the QE measurements is the calculation of the conversion gain. When the detector is read out it stores the signal in its pixels as analog-to-digital units (ADU). The conversion gain is used to convert the ADU values from each pixel to a number of electrons. The calculation of the gain and its effect on quantum efficiency will be further discussed in section 5.5. The shape of the graph is another attribute of the QE, although it is not as important as the actual QE values. For the data in Figure 5.3, the variation of the QE with wavelength is satisfactory, demonstrating a reasonably flat shape.

The above results only show an average QE value for each wavelength. It is important to look at the histogram of each wavelength to understand how the QE varies across the detector. The standard deviation of the QE fluctuation across H2-103 varied for different wavelengths from 1.5-2.5% . Recall that the goal of SNAP is to achieve 1% uniformity across the detector. The color maps provided are an important feature of the QE analysis. They present the QE as an image allowing the observer to see how the QE fluctuates spatially. Light patterns and detector non-uniformities are easily recognized and very helpful in understanding the process of a measurement and factors influencing the QE measurement of a device.

5.2 Scattered Light

The issue of scattered light in the quantum efficiency setup is one of great significance. It is crucial for the light distribution in our system must remain completely unaltered by sources of scattered light. The elimination of scattered light is a task that must constantly be monitored. I performed a measurement which used separate methods of producing dark images to test whether there was any scattered light in the QE setup. A standard dark image is produced by blocking all light from entering the setup, and then taking an exposure of the detector. However it is impossible to tell if scattered light reaches the detector during this measurement. One way to take a dark measurement and ensure that no scattered light reaches the detector is to place a circular, black-coated blocking mask between the integrating sphere port and the entrance to the dewar. The block I used covered an area the size of the entrance to the dewar and was aligned roughly halfway between the integrating sphere and the detector. Using this setup no scattered light could reach the detector. A dark image must be taken for each wavelength.

If there is scattered light in our system, the standard dark measurement would actually be measuring the dark current plus scattered light. When the dark image and current are subtracted from the illuminated exposures, scattered light included in the dark measurement also gets subtracted. However with the new dark measurements, no scattered light gets subtracted, since no scattered light was measured. This means that the illuminated frames analyzed using the new dark measurements would contain all scattered light data in the final QE results. If scattered light is in fact present, then the QE measurements using the new dark images are expected to be higher than the QE measurements using the standard dark images. The results of this test are shown in Figure 5.4.

The same set of illuminated exposures was used to compute both data sets; the only difference between the two QE measurements was the dark exposures used. The two QE results agree nicely with each other, signifying that there is no scattered light in our QE setup. For the wavelengths of interest (1000-1760nm), the largest variation between data sets was 1.6% at 1550 nm.

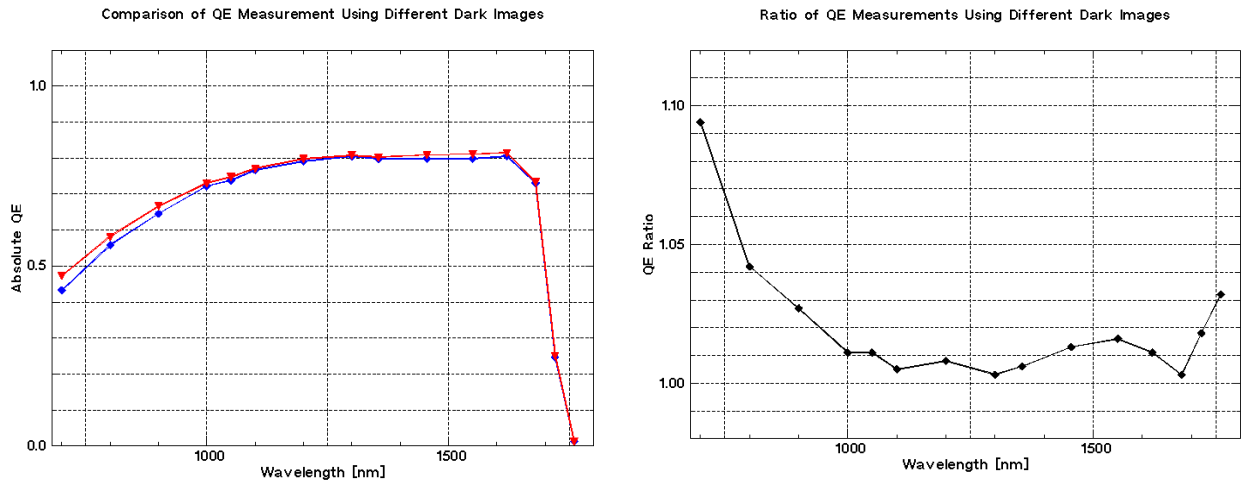


Figure 5.4: Left panel: QE data analyzed using two different dark images. The standard data taking method is in blue, and the data using the new dark measurement is in red. Right Panel: The ratio of the two QE curves. The agreement of the two curves provides strong evidence that scattered light in the QE system has been eliminated.

5.3 Uniform Light Distribution

Having a thorough understanding of the light distribution across the plane of the detector is a difficult task. Recently a movable stage was installed in the dewar that can be operated manually while the NIR detector and photodiode are mounted in the dewar. QE measurements versus the vertical position of the NIR detector and photodiode have been extremely useful in understanding the light distribution. Measurements of the photodiode (PD) current versus vertical position have recently shown that a flat field illumination exists in the plane of the detector (Figure 5.5). For the measurements taken there was a plate with a large window placed in the dewar. This allowed images of the detector to be taken without blocking any large portions of the detector as the stage was moved. From the data, it is apparent that the light levels do not change with vertical position. The first data set was taken in the normal position, and then the detector and PD were moved up by a $\frac{1}{4}$ " in each succeeding measurement. From Figure 5.5 it can only be concluded that there is a uniform light distribution over a $\frac{3}{4}$ " vertical range. With the addition of a few other measurements, it can be shown that a flat-field illumination is present across the whole area of the detector and photodiode.

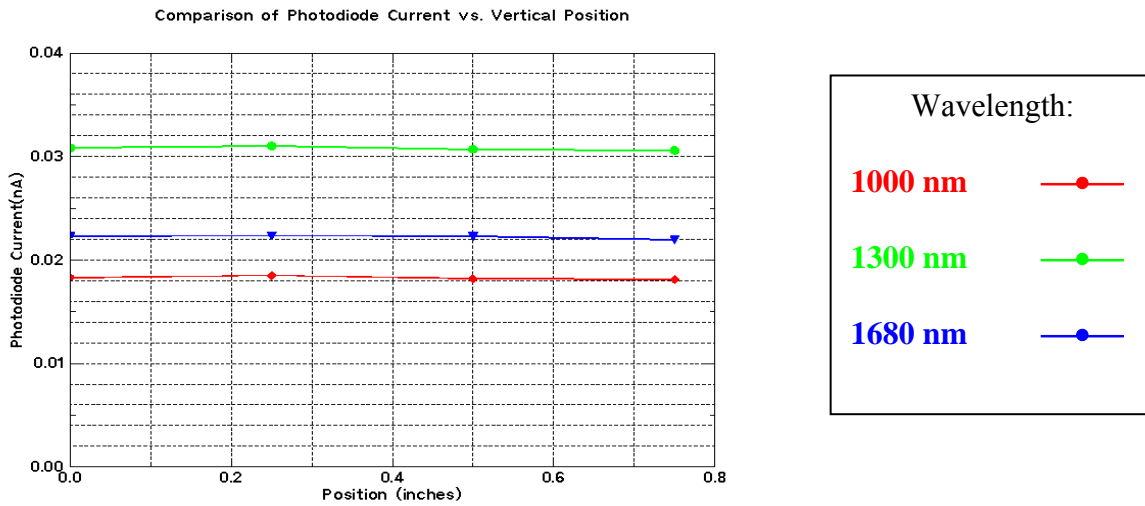


Figure 5.5: Photodiode current at three wavelengths, 1000 nm, 1300 nm, and 1680nm, for four different vertical positions. The photodiode current is independent of position.

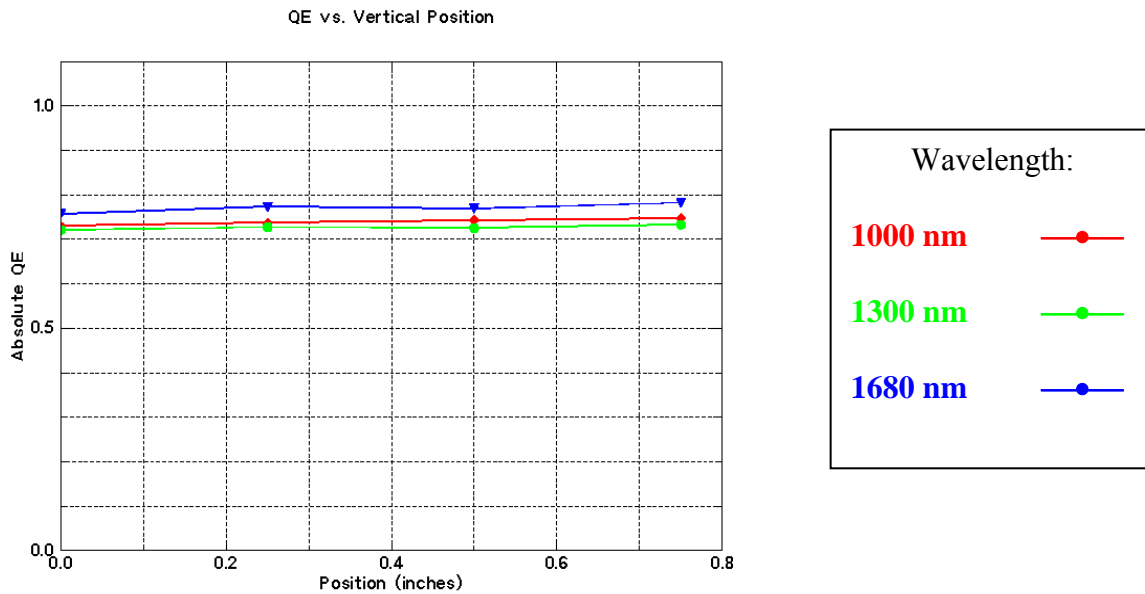


Figure 5.6: QE measurements at three wavelengths, 1000 nm, 1300 nm, and 1680nm, for four different vertical positions. The graph shows that the QE is independent of position.

As the detector moves in the vertical direction, the QE remains unchanged. It is already known that the PD current is the same for each position dependent QE measurement. If the QE varied with position, then it would be obvious that the light distribution is not a flat field, however this is not the case. The QE measurements in Figure 5.6 are only an average, and thus do not provide any concrete evidence of a uniform light field across the detector. To see how uniform the light field is, I have provided two color maps of H2-103 positioned at 0" and 3/4" at 1000 nm (Figure 5.7).

The color QE map allows one to quickly find patterns on H2-103. The left edges of the detector images below correspond to the top edge of the detector while it is in the dewar. The image on the right panel shows a QE of 0 at its left edge. This is because when the detector is raised up $\frac{3}{4}$ " in the current dewar setup, the top edge is blocked by a metal plate. There are bad pixels which show up as black or white on the color map, and scratches on the detector. We speculate that the non-uniform appearance in QE is not from non-uniform illumination, but from variations in the AR coating. Despite the change in position of the detector, the QE maps remain the same. It is easiest to see this by looking at the cyan pattern near the top, left corner of the detector. This means that the fluctuations seen on the images below are characteristic of H2-103, and not caused by non-uniform light. If the pattern on the left panel image was due to higher light levels towards the center of the detector, then this pattern would appear to be shifted to the right for the image on the right panel. Due to the high level of agreement between QE map images, along with practically identical PD currents versus position, it can be concluded that the pattern shown below is the true response of the detector and the light distribution across the detector and photodiode is a flat field. A subtraction of the two fits images in figure 5.7 was performed to better show the uniformity of light in this region. It is clear from the subtraction image in figure 5.8 that the light distribution is a flat field.

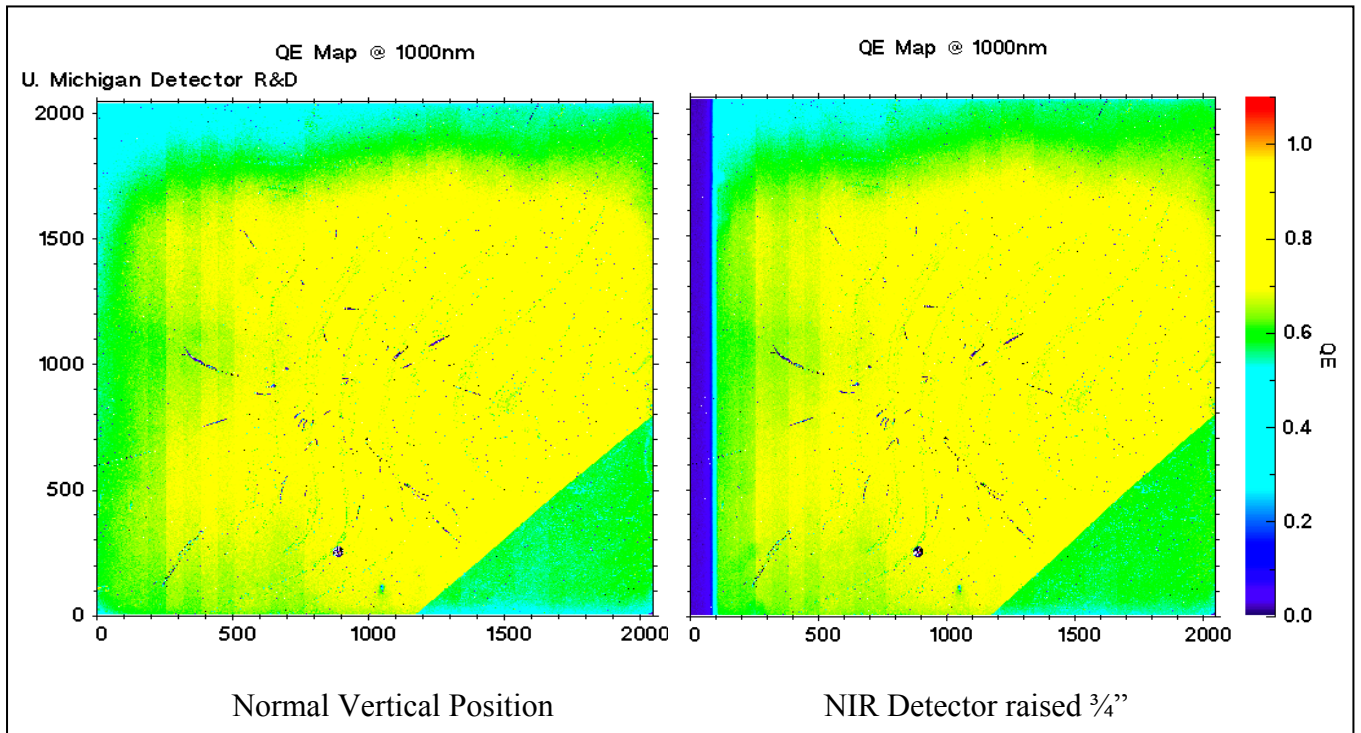


Figure 5.7: Comparison of two color QE Maps at different positions. The PD current was the same for both measurements. From the comparison, it can be concluded that the light distribution does not vary with position and is therefore a flat field for the current test conditions.

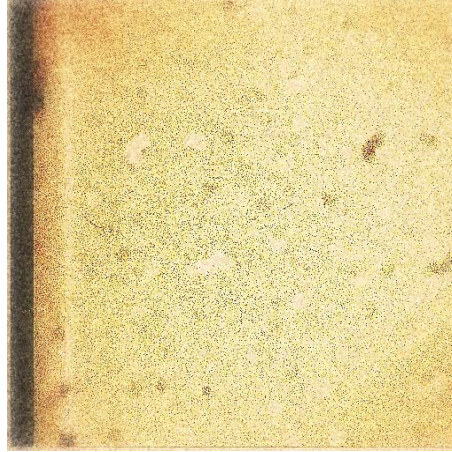


Figure 5.8: An image showing the subtraction of two QE images taken at different positions. The smoothness of the image demonstrates a uniform light field.

5.4 Conversion Gain

The conversion gain, g_c , is a conversion factor of electrons/ADU and is necessary to compute the QE. The signal in each pixel of an exposure is stored as ADU and therefore must be converted to electrons. All you need to calculate a rough gain measurement is an exposure that contains flat areas of data. The value of g_c is equal to the slope of a variance versus mean line. To calculate g_c , I took three subsections of a detector that were highly uniform. The subsections must be flat, otherwise the standard deviation and variance will not carry the appropriate information for the gain measurement. Calculating the mean and variance for each area will provide three data points that should all fall on the same line. If they are not on the same line, this means the area selected was not flat enough. The slope of the line is the value of the g_c . I calculated a value of $g_c = 1.59$ (Figure 5.9).

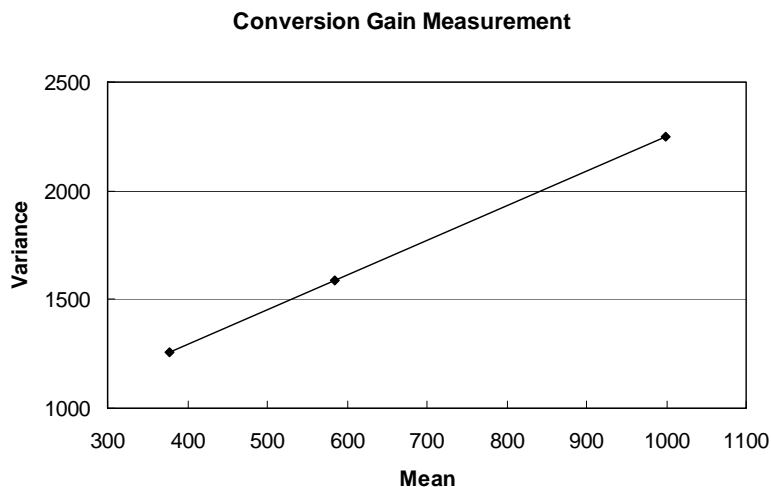


Figure 5.9: Plot of a conversion gain measurement. Three data points were computed from the mean and variance of three subsections. The slope of these points is the conversion gain.

5.5 Repeatability

It is important to be able to reproduce measurements. The reproduction of QE measurements is an area that needs improvement. The QE system had been completely re-modified at the beginning of 2007, and it took one year until all modifications were completed. It has been less than 5 months since the new QE setup has been working. In these past 5 months, measurements have been taken and analyzed for the purpose of thoroughly understanding every aspect of the new QE system. Now that sufficient analysis has been performed on the QE system, the focus of the QE measurements will shift towards getting repeatable data.

I compiled recent data of the PD currents (Figure 5.10) to see how the signal compared from day to day. The graph below demonstrates a consistent PD measurement from one day to the next. The data demonstrates very good repeatability.

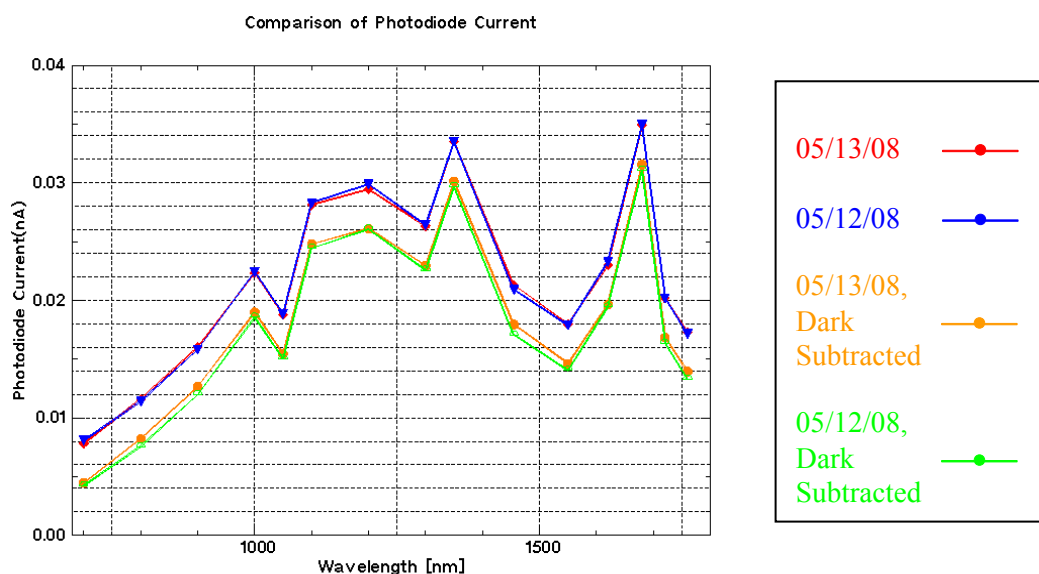


Figure 5.10: Measurements of the photodiode current taken over two consecutive days. The data shows a nice consistency.

A lot of analysis for the QE setup has gone into understanding how light behaves in the black box. The next step is to understand how the light behaves inside the dewar, especially for the different cold plates used inside the dewar. Repeatable measurements are very important. If a measurement returns new data each time, then there can not be any confidence in the measurement. In order to produce repeatable measurements, all aspects of the QE process must be thoroughly understood; otherwise one can not properly analyze the data and go forward with the next measurement.

The progress made in the past couple months of the QE analysis has been significant. Every measurement is a valuable contribution to the further understanding of quantum efficiency behavior for NIR detectors. Now that most major kinks have been worked out in QE setup, I am confident that we will be able to produce high-quality, repeatable quantum efficiency measurements.

Bibliography

- [1] Barron, Nathaniel, ‘Characterizing SNAP NIR Photodetectors with the Spot-O-Matic.’ 2006
- [2] Borysow, Michael, ‘Spot-o-matic: A Test Bed for Measuring Intrapixel Variation in Near Infrared Focal Plane Arrays.’ 2004.
- [3] Carroll, S.M., “Why is the Universe Accelerating?,” 2003.
- [4] Janesick, James R., ‘Scientific Charge-Coupled Devices.’ SPIE Press: 2001.
- [5] SNAP Collaboration, ‘SuperNova Acceleration Probe (SNAP),’ < <http://snap.lbl.gov/>>
- [6] ‘SuperNova/Acceleration Probe – Fact Sheet,’ <[http://snap.lbl.gov/pdf files/snapfacts.pdf](http://snap.lbl.gov/pdf_files/snapfacts.pdf)>